The conformational heterogeneity of the tumor suppressor p53 is tuned by punctual mutations

Anna Rita Bizzarri[1]

[1]Universita degli Studi della Tuscia Dipartimento di Scienze Ecologiche e Biologiche

July 19, 2022

Abstract

Conformational heterogeneity of the p53 tumor suppressor, wild-type and mutated forms, was investigated by computational modelling combined with all atoms Molecular Dynamics (MD) simulations. Four different punctual mutations (p53R175H, p53R248Q, p53R273H, p53R282W), which are known to affect the DNA binding and belong to the most frequent hot-spot mutations in human cancers, were taken into consideration. The MD trajectories of the wild-type and mutated p53 forms were analysed by Essential Dynamics, to extract relevant collective motions. The same trajectories were also analysed by the frustration method which allows to evaluate the degeneracy of the energy landscape. We found that punctual mutations can modulate the collective motions of p53 at different extent according to the specific mutation. Furthermore, mutations can affect the frustration level of p53 specially in the regions involved in the binding to physiological ligands. The regions of p53 with larger collective motions are also characterized by a high frustration level. The regions of p53 characterized by a high frustration level are also largely involved in wide collective motions. Such a correlation is discussed in connection with the intrinsic disordered character of p53 and also with its central functional role.

The conformational heterogeneity of the tumor suppressor p53 is tuned by punctual mutations

Anna Rita Bizzarri

Biophysics and Nanoscience Centre, DEB, Università della Tuscia, Largo dell'Università, 01100, Viterbo, Italy

Abstract

Conformational heterogeneity of the p53 tumor suppressor, wild-type and mutated forms, was investigated by computational modelling combined with all atoms Molecular Dynamics (MD) simulations. Four different punctual mutations (p53R175H, p53R248Q, p53R273H, p53R282W), which are known to affect the DNA binding and belong to the most frequent hot-spot mutations in human cancers, were taken into consideration. The MD trajectories of the wild-type and mutated p53 forms were analysed by Essential Dynamics, to extract relevant collective motions. The same trajectories were also analysed by the frustration method which allows to evaluate the degeneracy of the energy landscape. We found that punctual mutations can modulate the collective motions of p53 at different extent according to the specific mutation. Furthermore, mutations can affect the frustration level of p53 specially in the regions involved in the binding to physiological ligands. The regions of p53 with larger collective motions are also characterized by a high frustration level. The regions of p53 characterized by a high frustration level are also largely involved in wide collective motions. Such a correlation is discussed in connection with the intrinsic disordered character of p53 and also with its central functional role.

Keywords: p53, mutated p53, Molecular Dynamics Simulations, collective modes, energy landscape

INTRODUCTION

p53, often called tumor suppressor protein, plays a crucial role in several biological functions, such as cell cycle progression, apoptosis induction and DNA repair.[1] p53 is a homo-tetrameric protein, with each monomer consisting of a N-terminal transactivation domain (NTD), a C-terminal domain (CTD), and a large structured region core domain (DBD\sout)) which binds DNA response elements.[2–5] The p53 activity is finely tuned by different processes, including a direct interactions with some molecules, such as MDM2, S100, COP1 and, interestingly, miRNA.[6,7] When p53 does not work properly, for example as consequence of a mutation, a drastic increase of diseases, such as cancers, may occur.[8] In more than half of human cancers, mutations are located in the DBD portion;[9–11] this can strongly alter the capability of p53 to perform its tumour suppressive functions and sometimes leads p53 to acquire new functions, (gain-of-function, GOF) including transcriptional activation of different genes.[12] p53 is characterized by the presence of some structurally disordered regions which prevent the biomolecule from a full 3D characterization.[13]Accordingly, p53 belongs to the class of intrinsically disordered proteins (IDP), whose partial structural disorder gives rise to the co-existence in solution of slightly different conformations.[14] Such a heterogeneity confers to these systems the capability of performing different functions, often through the binding to different biological molecules.[15,16]

From a physical point of view, IDPs can be described within the Frauenfelder's framework which represents the protein energy landscape as being characterized by several nearly isoenergetic local minima; with such a picture being reminiscent of that describing other complex systems, such as glasses, spin glasses, etc.[17,18]Briefly, competing interactions among components do not allow these systems to reach a global minimum, instead a plethora of local minima emerge and are explored during the functional dynamics.[19] Additionally, it is assumed that protein molecules have evolved following the principle of minimal degeneracy, or frustration, for which the energy of a protein progressively decreases as far as it approaches its native state;[19] with some residual frustration being present to facilitate fundamental biological functions.[20] In this framework, IDPs constitute a particular class of proteins whose partial disorder introduces a further contribution to the frustration of the energy landscape.[21]

For its prominent biological role, p53 is an extremely intriguing example of IDPs whose understanding deserves a large interest from both the biological and physical point of view. With the aim to investigate the energy landscape of p53, we have applied a computational approach to wild-type p53 (p53wt) and four p53 molecules; with each one bearing a punctual mutation. Preliminarily, a model for the whole structure of the p53wt monomer and of four mutants have been derived by combining available information from Protein Data Bank (PDB), with previously developed approaches.[22] All these p53 systems have been then submitted to molecular dynamics (MD) simulations and the resulting trajectories have been analysed by two methods: Essential Dynamics (ED) and frustration analysis. ED method, based on Principal Component Analysis (PCA), allows to extract collective modes from the conformational space explored by a biomolecule during the MD runs. Upon the assumption that the major collective modes dominate the functional dynamics, ED is widely used to extract motions which could be relevant for the protein functionality. Furthermore, frustration analysis, based on an energy landscape-inspired theory, allows to investigate the energetic degeneracy of protein molecules. Accordingly, protein sites with high local frustration are expected to correlate with functional regions related to both binding sites and regions involved in allosteric transitions.[23]

We have analysed wild type p53 (p53wt), and four punctual mutations (p53R175H, p53R248Q, p53R273H, p53R282W), which are part of mutations that affect DNA binding and belong to the most frequent hot-spot mutations in human cancers.[24–27] p53R175H, in which Arg175 is replaced by His, is one of the most common p53 mutants found at progressively higher quantities in several tumors, such as lung, colon and rectal and with a particularly high incidence in breast tumor[28–30]. Such a mutation abolishes the p53wt ability to recognize its target genes involved in tumor suppression, yet promotes new GOF functions, through direct or indirect associations with DNA [28,31]. P53R248Q, in which Arg248 is replaced by Gln, is one of the most common mutants found in breast cancers and its presence is also largely used as patients death predictor.[32] This punctual mutation yields a weakness of the binding to DNA with a concomitant increase of aggregation propensity.[33] The p53R273H mutant, in which Arg273 is replaced by His, is characterized by a reduction of the DNA binding and it is associated to an inhibition of the autophagy machinery, promoting cancer cell survival.[34] Finally, the p53R282W, in which Arg282 is replaced by Trp, is associated with shorter survival

time. This mutant still retains partial transcriptional ability, however it exhibits a significant aggregation propensity.[33,35]

Our analysis has put into evidence the presence of wide collective modes and a rather high degeneracy level of energy landscape, in p53, consistently with its complex structural character which is at the basis of its extremely rich functional role. Punctual mutations can significantly modulate both collective modes and degeneracy level of p53; the results suggesting a close interplay between these two aspects, which deserves further investigations.

COMPUTATIONAL METHODS

2.1 Modeling of p53 molecules

The model of the full-length wild-type p53 monomer was built from the aminoacid sequence using the I-TASSER suite[36,37]including the B chain of DBD portion in complex with a consensus DNA (1 TUP entry from the protein data bank).[5] The predicted protein structure was characterized by a medium confidence with a C-score 2.37 and a TM score of 0.44 -0.14, for Model 1. According to ref.[22], we assumed that Model 1 provides a realistic starting point for the MD simulation to investigate the intrinsic flexibility of p53. The Zn ion, which is tetrahedrically coordinated to the side-chains of Cys176, His179, Cys238, and Cys242, forms a Zn-finger motif connected to the L_2 and L_3loops.[38] The interaction of the Zn ion with its ligands was treated through a bonded approach in which the Zn-N and Zn-S bonds and S-Zn-S angles, were set according to the parameters provided in refs.[39–42] Punctual mutations were inserted by the Swiss PDB Viewer software starting from the p53wt model.[43] In particular, in p53R175H, Arg175 was replaced by His; in P53R248Q, Arg248 was replaced by Gln, in p53R273H, Arg273 was replaced by His, and finally, in p53R282W, Arg282 was replaced by Trp.

2.2 Molecular Dynamics (MD) simulations and analysis

MD simulations of wild-type and mutated p53 molecules in water were carried out by the GROMACS 2018 package [44] using AMBER03 and SPC/E Force Fields for the protein [45] and for water [46], respectively. Each p53 molecule was centered in a cubic box of edge 9.0 nm, filled with water molecules to assure a minimum hydration level of 8 g water/g protein. The ionization states of protein residues were fixed at pH 7, and 36 water molecule were randomly substituted with an equal number of Na^+ions to keep the systems electrically neutral. Simulations were performed by following the same procedures used in refs.[42,47] Briefly, the Linear Constraint Solver (LINCS) algorithm was utilized to constrain H bonds,[48]while the electrostatic interactions were computed using the Particle Mesh Ewald (PME) method with a lattice constant of 0.12 nm.[49,50] Each system was submitted to an energy minimization procedure by using the steepest descent method. After minimization, the system was heated to 300 K with steps at 50,100,150 and 250 K and submitted to a 50 ns long MD trajectory for equilibration at 300 K, followed by further 150 ns for data collection. Periodic Boundary Conditions in the NPT ensemble with T=300 K and p=1 bar, with a time steps of 2 fs were used. The temperature was controlled by the Nosé-Hoover thermostat with a coupling time constant t_T=0.1ps[51] while the Parrinello-Rahman extended-ensemble, with a time constant t_P= 2.0 ps, was used to control pressure.[52] For each system (wild-type protein and mutated forms), five independent runs were performed and MD trajectories were analysed by the GROMACS package tools.[44] The temporal evolution of the resulting trajectories was monitored by following the Root Mean Square Displacement (RMSD), the Root Mean Square Fluctuation (RMSF), the Surface Accessible Surface Area (SASA), the gyration ratio (R_g) according to the methods described in ref.[53] The figures were created with Pymol and VMD.[43,54]

2.3 Essential Dynamics (ED) analysis

The MD trajectories were analysed by PCA and in particular by the ED method implemented in GROMACS.[55,56] Such an approach identifies a new reference frame to describe the overall dynamics of the system, allowing to extract the protein motions which are mostly contributing to the overall dynamics. [57] ED was carried out by the Covar and Anaeig subroutines of GROMACS.[55,56] After a least square fit to remove roto-translations, the covariance matrix C_{ij} was calculated by:

$C_{ij} = \langle (x_i - \langle x_i \rangle)(x_j - \langle x_j \rangle) \rangle$ (1)

where x_i are the x,y,z Cartesian coordinates of the C_α atoms of DBD and <> indicates an average

over the trajectories. C_{ij} was diagonalized by finding out a set of eigenvalues and eigenvectors; with the eigenvectors corresponding to directions in a N dimensional space and are called principal coordinates (PCs), while the eigenvalues represent the total mean square fluctuations along the corresponding eigenvectors.

2.4 Frustration analysis method

The energy landscape of p53 molecules was investigated by applying the algorithm implemented in the Protein Frustatometer 2 Server (*http://frustratometer.qb.fcen.uba.ar/.*) The frustration index ($F_{i,j}^{m}$), or Z-score, for the contact between the aminoacids i,j, was calculated through the following expression: [58,59]

$$F_{i,j}^{m} = \frac{E_{i,j}^{N} - \langle E_{i,j}^{U} \rangle}{\sqrt{1/N \sum_{k=1}^{n} \left(E_{i,j}^{N} - \langle E_{i,j}^{U} \rangle\right)^2}} \quad (2)$$

where $E_{i,j}^{N}$ and $E_{i,j}^{U}$ are the pairwise interaction energies of the molecule in the reference (U) and in the decoy configuration (N), respectively; $< E_{i,j}^{U} >$ being the average energy of the decoys. For the analysis, a region of 5 Å from the C_α-atom for each residue was used. The energy distribution of the decoy was calculated using the configurational frustration in which the native interaction between two residues was measured by randomly selecting aminoacids from the protein composition and even by changing in location. The energy includes the electrostatics with the k constant fixed at 4.15 which corresponds to a relative electric constant of 80. The frustration index of the p53 structures, was calculated by averaging 100 snapshots sampled in the last 10 ns of the 150 ns-long runs.

RESULTS AND DISCUSSION

3.1 Analysis of general properties

Fig.1 shows the best model for the structure of the p53wt monomer (see Methods Section) with the four aminoacids submitted to a mutation represented as coloured spheres. All these residues are located in the northern part of the molecules and they are clustering around the Zn ion which is involved at the DNA binding region.

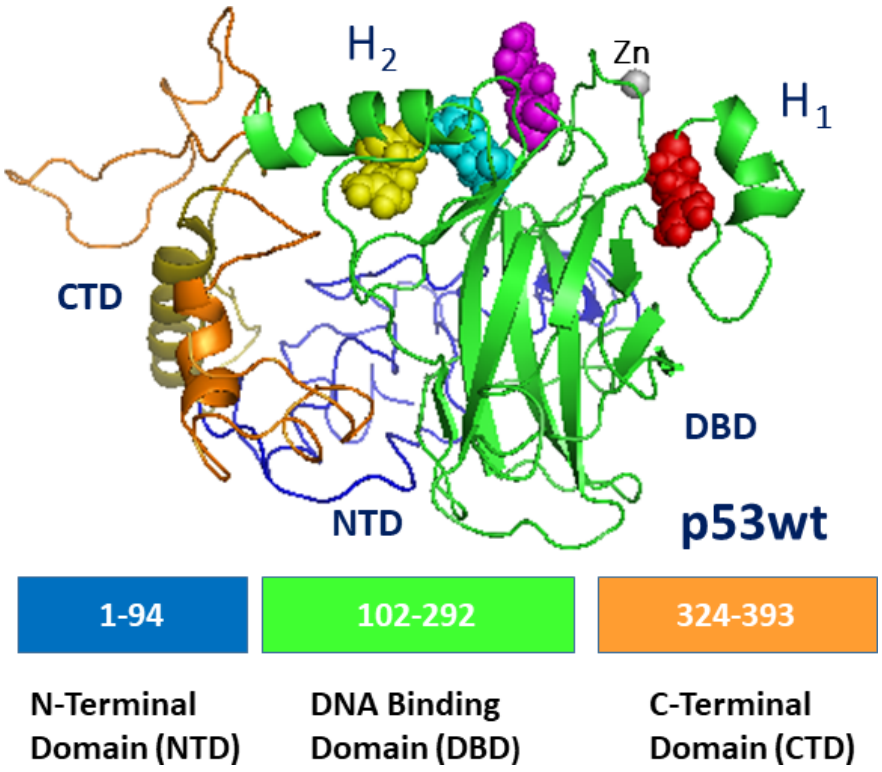

Figure 1. Graphical representation of the best model for p53wt monomer. The residues submitted to a punctual mutation are represented as coloured spheres: p53R175H (red), p53R248Q (cyan), p53R273H (yellow), p53R282W (magenta). The Zn ion is represented as a light grey sphere. The various p53 domains are marked in different colours.

Fig.2A shows representative temporal evolution curves of all atoms RMSD, during a 150 ns-long MD trajectories. In all the cases, we note a rather rapid increase within the first 5 ns, followed by a slower increase which is practically completed within the first 50 ns. Then, the RMSDs oscillate around a plateau; with this indicating the establishment of a substantially stable state. The observed trend is qualitatively similar to that usually detected in the RMSD of other proteins, however, the time required to reach a plateau is generally longer, indicating the requirement of more time for the relaxation of the molecule from its initial state. Additionally, the rather high RMSD values reached at the end of the run (ranging from 0.4 to 0.8 nm), find a correspondence with the presence of some disordered regions which confer to the protein molecule a higher flexibility.

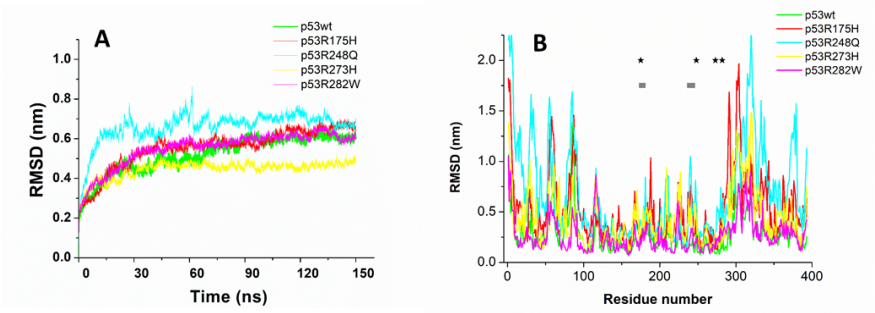

Figure 2. A) Temporal evolution of the RMSDs for all the p53 systems. B) RMSD as a function of the residue number. Positions of the residues undergoing a mutations are marked by black stars, while those of residues involved in the DNA binding are marked by grey squares.

The average and the corresponding standard deviation, of the RMSD, SASA and R_g, for the five p53 systems, are reported in Table 1. p53R248H shows a higher RMSD value with respect to p53wt, while the RMSDs of the other mutants are rather similar among them and even to that of p53wt. Additionally, both the gyration radius, R_g and the SASA values of all the mutated forms are almost equal to those of p53wt. Finally, the fraction of the aminoacid residues involved into secondary structure, averaged from the last 10 ns of the runs, is practically the same for all the p53 forms. This means that the analysed mutations do not strongly affect the structure of the molecule.

Table 1. General properties of p53wt and the four p53 mutants. RMSD, SASA and R_g were evaluated from the 50-150 ns interval of the run, while the percentage of the secondary structure was evaluated from the average structure from the last 10ns (141-150 ns).

System	RMSD (nm)	SASA (nm^2)	R_g (nm)	Secondary Structure (%)
p53wt	0.50 ±0.06	216± 6	2.22±0.05	64±6
p53R175H	0.53±0.06	215± 6	2.26±0.04	63±8
p53R248Q	0.71±0.05	220± 3	2.26±0.04	67±9
p53R273H	0.46±0.04	214± 4	2.24±0.05)	64±8
p53R282W	0.54±0.05	217± 5	2.25±0.05	65±7

Fig.2B shows representative RMSDs as a function of the residue number, for all the systems; the position along the chain of mutations being marked by black stars, while grey squares indicate positions of aminoacids directly involved into the DNA binding. The largest part of RMSD peaks is located at almost the same position in the various curves, however, the peak intensity can significantly vary among them. p53R248Q generally exhibits higher RMSD values with respect to those of p53wt, as expected. Notably, the aminoacid residues involved in the DNA binding are characterized by a rather high variability in the RMSD values; this suggesting possible alteration of region of the protein with possible slight changes in the DNA binding properties.

3.2 Analysis of p53 collective modes

The MD trajectories, in the temporal window of 51-150 ns, of wild-type and mutated p53 molecules have been investigated by the ED method to find out the relevant collective modes. The first 30 eigenvalues, extracted from the covariance matrix of the atomic fluctuations of representative runs, and ranked in a decremental order, are shown in Fig.3A. In all the cases, the eigenvalues rapidly decrease down to a very low value (less than 5% of the maximum), within the first ten eigenvalues. Similar results have been obtained for other trajectories. Such a trend, commonly observed in the eigenvalues of protein modes, indicates that the most relevant motions are concentrated in a few modes whose dimensionality is represented by the number of eigenvalues accounting for the first ranked values.

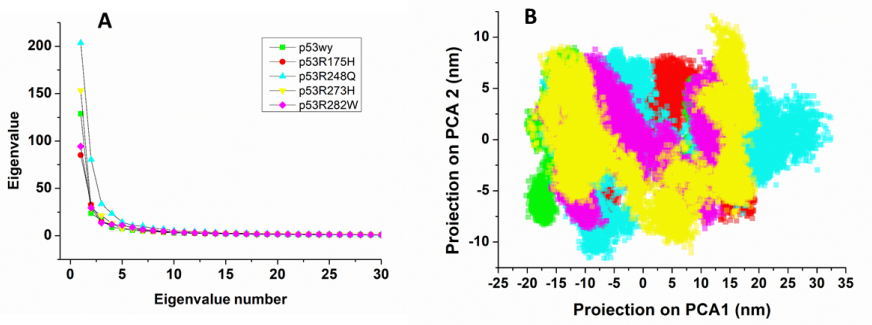

Figure 3. A) Eigenvalues as a function of the eigenvalue number; B) 2D-plot of projection of PC1 vs. the projection of PC2 for all the systems**.** Colours are the same as in Fig.1.

Table 2 reports the average percentages of the ratio between the sum of first ten eigenvalues over the sum of all ones (column 2). The first ten eigenvalues capture more than 60% of the total in all the cases, confirming that the dynamics of p53 is dominated by a few principal modes. No significant changes are observed among the various systems, indicating that the introduced mutations do not drastically affect the global dynamics of p53, consistently with the capability of these mutants to perform at least in part their physiological role.

Table 2. ED and frustration properties of the p53wt and of p53 mutants. ED parameters were derived from the 50-150 ns interval. Frustration index was evaluated from the average structure from the las 10 ns (141-150 ns).

System	Sum of first ten/sum of all (%)	Width PC1 (nm)	Width PC2 (nm)	Frustration index %
p53wt	67±8	35±2	22±4	7.3±0.6
p53R175H	62±3	31±2	24±1	8.6±0.7
p53R248Q	71± 7	49±7	32± 4	8.9±0.9
p53R273H	66±8	38±3	26± 3	8.2±0.6
p53R282W	62± 9	31±2	24±2	7.8±0.9

Based on these results, global information about the configurational space sampled by the p53 systems, can be derived from the first ranked eigenvectors. Representative 2D-plots of the projection on the first eigenvector (PC1) vs. the second one (PC2) are collectively shown in Fig.3B by using coloured spots. In all of the cases, the spots cover a wide region indicating the establishment of wide collective modes in both wild-type and mutated p53 molecules. The covered width of PC1 and PC2, averaged over all the runs, are reported in Table 2. Notably, for p53wt, the width values are higher with respect to those previously found for the DBD portion of p53 (of about 15 nm) [60]. This clearly indicates that wider collective motions are established in p53wt with respect to its DBD portion; with this being likely put into relationship to the presence in whole p53 molecule of the CTD and NTD regions (missing in DBD) which confer to the molecule a higher flexibility. Indeed, these regions, being devoted to interact with several different ligands, would require some heterogeneity for performing this "hub-like" function.

PC1 and PC2 of p53R248H and p53R273H cover a wider region in comparison with those of p53wt, while they have almost the same extensions for p53R175H and p53R282W. Accordingly, punctual mutations could modulate collective modes of p53; with these changes likely impacting on the capability of this protein to interact with some ligands.

To closely address the effects of punctual mutations on collective motions in the various part of the p53

molecule, we have analysed the snapshots of the extreme projections on the eigenvectors. Representative snapshots of the extreme projections on the first two eigenvectors of p53wt are shown in Fig.4A and Fig.4B. In both the cases, we note the presence of collective modes throughout the whole protein structure; whose extension, however, varies from region to region of the protein. As expected, wider displacements are detected for the first eigenvector with respect to the second one. The largest displacements appear within both the random coils and α-helices located at the CTD and NCT portions. Since these parts of p53 are largely involved in the binding to different partners, such a result may point out a functional role of the related collective motions. Additionally, the rather restricted collective modes in the regions involved in β-sheets is consistent with the fact that they provide the skeleton of the molecule, whose structure should be preserved for a higher stability.

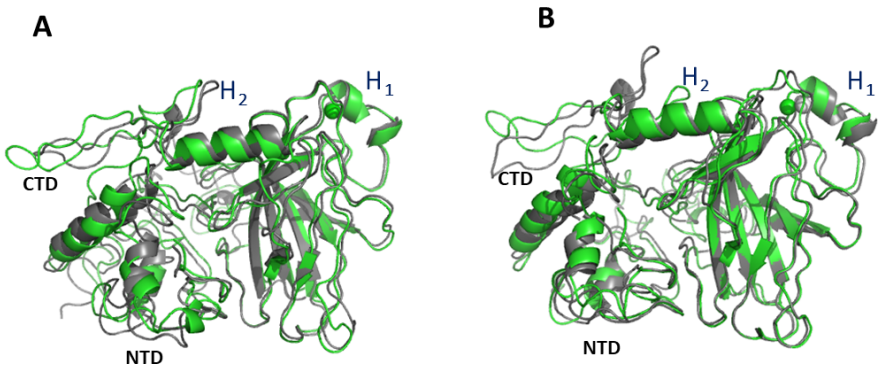

Figure 4. Extreme trajectory conformations projected along: A) the first; and B) the second eigenvector for p53wt. The Zn ion is represented as a sphere.

The region close to Zn ion, which is involved in the DNA binding, is also characterized by small collective motions. It could be speculated that the occurrence of restricted modes in this part could favour an optimized interaction with DNA; similar results having been obtained for the collective motions of the other runs of p53.

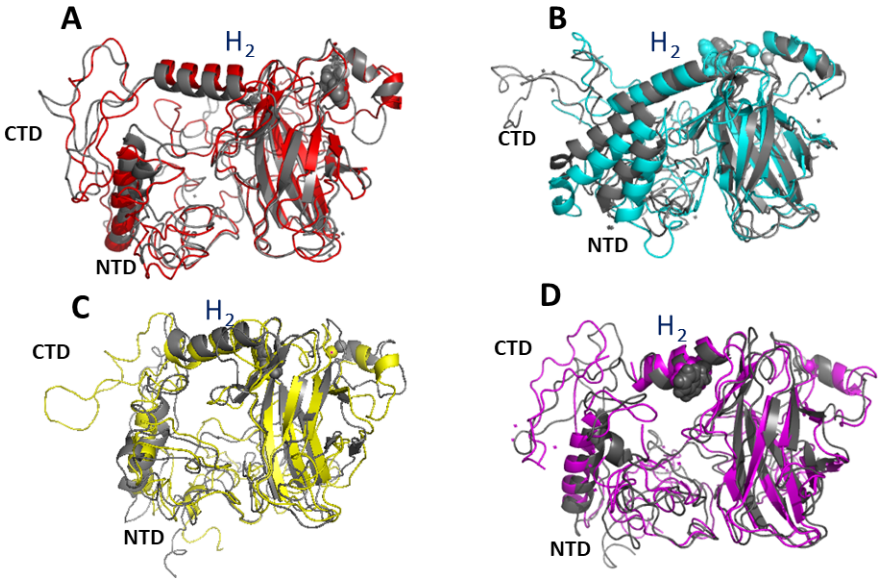

Figure 5. Extreme trajectory conformations projected along the first eigenvector for the four mutated p53

molecule. A) p53R175H; B) p53R248Q; C) p53R273H; and D) p53R282W. Mutated residues and Zn ion are represented as spheres.

Figure 5 shows representative snapshots of the extreme projections on the first eigenvector for the four mutated p53 molecules. Similarly to what observed for p53wt, rather wide collective modes are detected at both random coils and α-helices, while the β-sheets are involved to a lesser extent. At visual inspection, the amplitude of the collective modes appears wider for p53R248Q (Fig.5B) with respect to those of the other mutants, consistently with what observed in the 2D-plot. In particular, this mutant exhibits wide collective motions at both the CTD and the NTD regions; with such a result finding a correspondence with the high propensity of these regions to form amyloid fibrils.[33] Indeed, the presence of wide collective motions widens the possible configurational landscape, and then it could increase the interaction capability of with additional molecular species. In this respect, it has been recently observed that changes around the mutation, may allosterically propagate to the CTD and NTD regions, from which fibril nucleation is believed to start.[33] Finally, both the p53R175H and p53R282W mutants (Fig.5A and D), show the presence of collective modes throughout the whole structure, with however rather low extension. Such a behavior is in agreement with the global effects on the p53 molecule observed as consequence of these two punctual mutations. Indeed, the corresponding mutations are susceptible to cause global conformational distortions which affect the binding of DNA, while the p53R248Q and p53R273H mutants are classified as contact mutants since their mutations affect the contact with DNA.[25–27]

Interestingly, the H_2-helix is involved in collective motions in all the mutants. Since it is also involved in the DNA binding, the presence of these collective motions could be put into relationship to the interaction with DNA in agreement with what has been experimentally observed for these mutants.[61] Finally, we note that the region around the punctual mutations shows some collective modes which are wider for both the p53R248Q and p53R273H mutants. Such an effect finds a correspondence with the local character of the effects observed for these two mutants, in which mutations mainly affects the region around them.[25–27] Generally, the establishment of new collective motions in mutants with respect to p53wt may engender new binding capabilities and then new functionalities in connection with the GOF hypothesis.

Therefore, the ED analysis on wild-type and mutant p53 molecules indicates the presence of wide collective modes through the molecule, with a large involvement of both random coils and α-helices in regions where the binding of ligands is expected; with this having a direct effect on the p53 response. The different punctual mutations can differently modulate collective modes with possible direct consequence on the p53 functionality.

3.3 Frustration analysis

The degeneracy or frustration of the energy landscape for wild-type and mutated p53 molecules has been investigated by applying the frustration analysis as described in the Methods Section. We have first performed a global analysis by evaluating the total frustration index, obtained by averaging over both all the residues and all the runs; these values being reported in Table 2. For p53wt, we found a frustration index of 7.3, while a higher value is detected for the p53R248Q. The other mutants have a frustration index which is almost the same of that of p53wt. Then, we have carried out a local analysis of frustration around each residue in the average structure of p53 molecules, as derived from the last 10 ns of the run.

Figs.6-10 show representative snapshots, and the related map, for the frustration of p53wt and of the mutated p53 forms. In the snapshots, connections between residues characterized by high frustration are marked by red dashed lines, while those with low frustration are marked by green dashed lines. Similarly, in the map, red spots indicate residues with a highly frustration, while green spots residues with low frustration. More specifically, spots along the diagonal provide connection between residues which are close along the chain, while spots out of the diagonal indicate spatially close residues but belonging to different part of the molecule. From a global visual inspection of all the snapshots, we note that a high frustration is often detected at random coils, and even at α-helices, although to a lesser extent in the latter. At variance, low frustration is observed at β-sheets.

For p53wt, three main clusters of red spots, labelled as C_1, C_2 and C_3 and marked by blue circles, can be visualized in the map along the diagonal (Fig.6B). Clusters C_1 and C_3 involve the random coils of CTD, while C_2 is at the H_1-helix. Other smaller clusters of red spots are detected along the diagonal. Additionally, some red spots can be also observed out of the diagonal. In particular, two small clusters, O_1 and O_2 (see red circles in Fig.6B), detected out of the diagonal, are related to connections between residues belonging to the CTD helices to the internal part of the molecule. Furthermore, the region close to Zn ion is also characterized by the presence of some frustration.

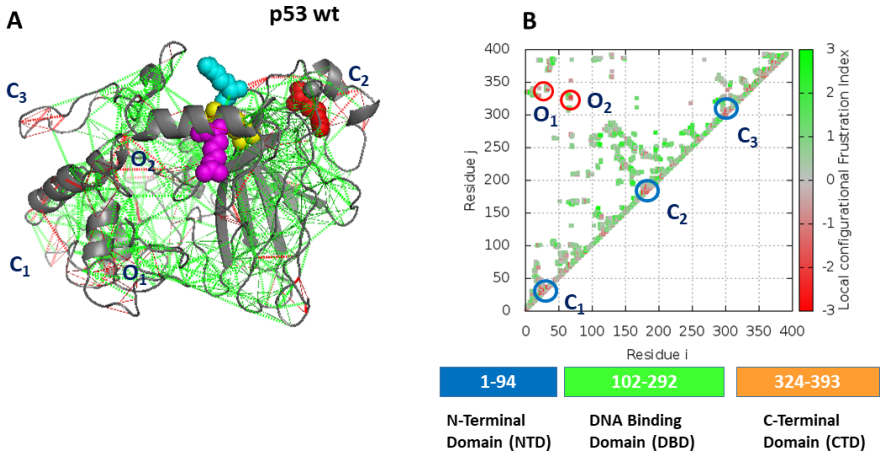

Figure 6. A) Frustration snapshot of p53wt.The level of frustration is represented by the coloured scale: green represents minimal frustration and red high frustration. The residues submitted to punctual mutations and the Zn ion are represented as spheres.

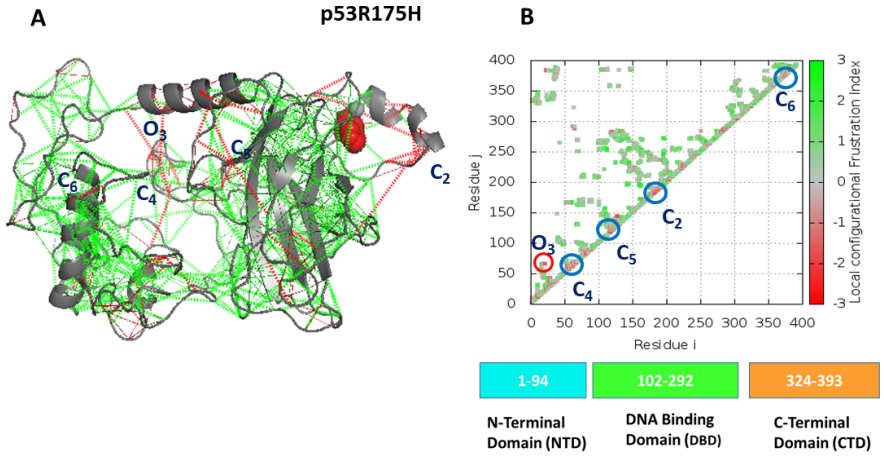

Figure 7. A) Frustration analysis of p53R175H. The level of frustration is represented by the coloured scale: green represents minimal frustration and red high frustration. The mutated residue (175H, red) and the Zn ion (grey) are represented as spheres.

For the p53R175H mutant, several red spots appear in the map along the diagonal, and four main clusters can be identified (Fig.6B). These clusters have a slighly lower density with respect to the clusters of p53wt. Only the C_2 cluster is shared with p53wt, while the other ones appear at different positions. Notably, at the CTD region, where the C_3 cluster has been detected in p53wt, no frustration appears. Since this region is involved in the binding of several ligand, such an effect could limit the p53R175H functionality with respect

to p53wt. Furthermore, the C_4 cluster, which is not visible in Fig.7A as being located in the back part, involves a random coil. A few spots are detected out from the diagonal and a single cluster, O_3, involving the H_2–helix, emerges.

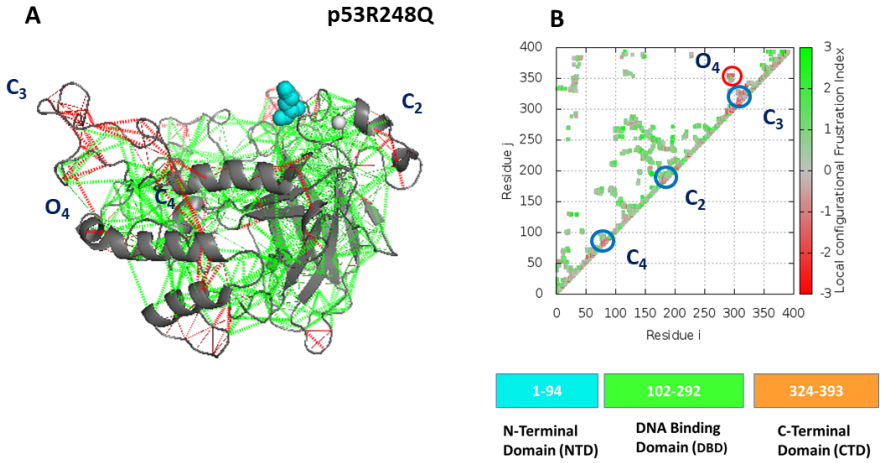

Figure 8. A) Frustration analysis of p53R248H. The level of frustration is represented by the coloured scale: green represents minimal frustration and red high frustration. The mutated residue (248H, cyan) and the Zn ion (grey) are represented as spheres.

The snapshot and the map of p53R248Q, shown in Fig.8, exhibit a rather high level of frustration, consistently with the high frustration index of this mutant, which, indeed, is also higher with respect to p53wt. In the map, several red spots along the diagonal can be observed; many of them having a higher density in comparison to those of the other p53 molecules. Three main clusters can be identified (C_2 and C_3 and C_4). C_2 and C_3 are shared with p53wt, while C_4 is shared with p53R175H. A few spots appear out of the diagonal; with the most significant, labelled as O_4, is related to the connection of different portions in the CTD part. The high frustation detected at the CTD part could be put into relationship to the high propensity of this regions to form fibrils. Indeed, a high frustration can give rise to several slighly different conformations which, in turn, could increase the possibility to interact with surrounding molecules.

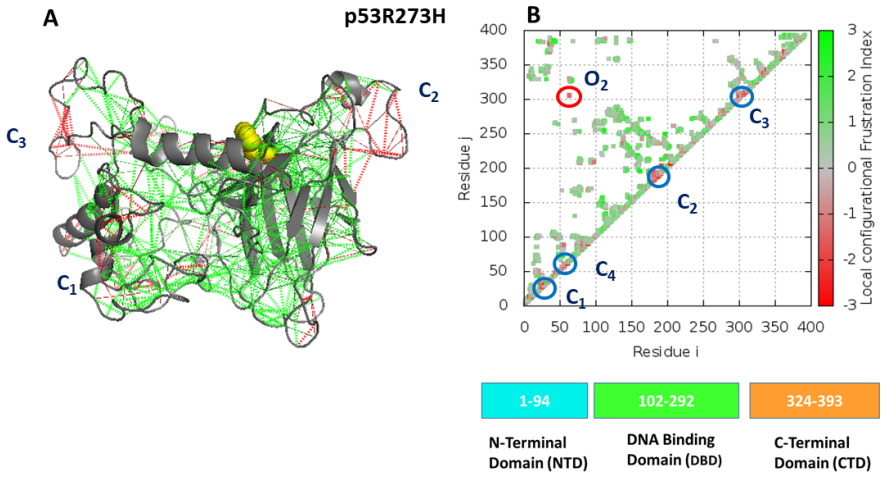

Figure 9. A) Frustration analysis of p53R273H. The level of frustration is represented by the coloured scale: green represents minimal frustration and red high frustration. The mutated residue (273H, yellow) and the

Zn ion are represented as spheres.

The snapshot and the map of p53R273H (see Fig.9) show a rather close similarity to those observed for p53wt. Indeed, the map exhibits the presence of the C_1, C_2 and C_3 clusters along the diagonal. A further cluster, C_4, shared with p53R175H, appears along the diagonal. Out of the diagonal, one cluster, O_2, is also shared with p53wt.

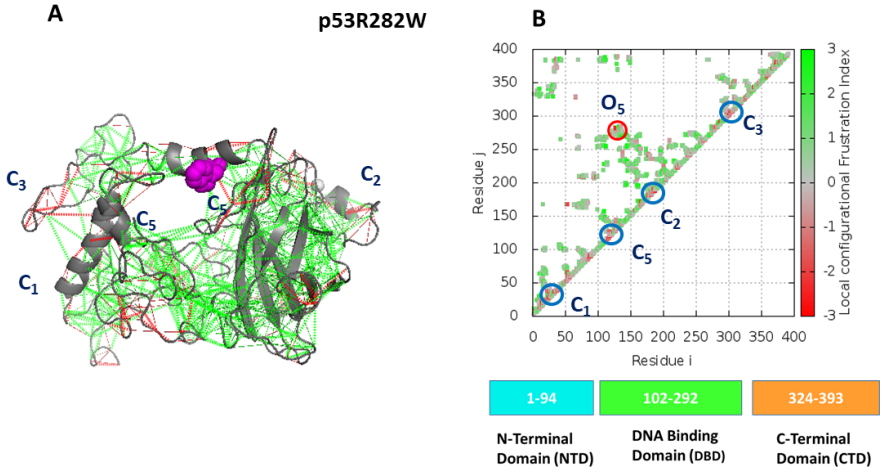

Figure 10. A) Frustration analysis of p53R282W. The level of frustration is represented by the coloured scale: green represents minimal frustration and red high frustration. The mutated residue (282W, magenta) and the Zn ion (grey) are represented as spheres.

Finally in the map of p53R282W (Fig.10B), we note the C_1, C_2 and C_3 clusters, which are shared with p53wt, and a further rather dense cluster C_5, shared with p53R175H. Some red spots out of the diagonal appear in the map. In particular, the cluster, O_5, involving the DNA binding region could induce some changes in the DNA binding properties.

These results put into evidence that regions of p53 characterized by a high level of frustration are largely those involved in binding with possible ligands. Such a result suggests that high frustration could play a role in functionality. Furthermore, the evidence that punctual mutations can locally alter frustration finds a correspondence with the capability of mutations to induce effects on the functionality. More generally, the fact that a punctual mutation can also modify frustration, even at regions far from the mutations, is in agreement with the complex character of this protein for which the global behaviour might be affected even by a tiny change of a specific region of the system.

Finally, it deserves some interest to discuss the results about frustration in connection with those of collective modes emerging form ED analysis. A comparison between the frustration level and the presence of collective motions in p53 molecule (see Fig.4 and Fig.6), puts into evidence that collective motions mainly appear in regions characterized by a high frustration. This can suggest a close interplay between high frustration and collective motions. As already mentioned, high frustration is related to the presence in the energy landscape of many nearly isoenergetic minima; with these minima corresponding to slightly different local arrangements of protein atoms (i.e. conformational states). On the other hand, a collective mode, globally involving various parts of the biomolecule, could be described as a collection of different conformational states involving different portion of the molecule; this being likely finalized to give rise to specific global structure of the protein molecule able to perform a specific role. In this picture, a high frustration index of a molecular portion could be a required condition to give rise to collective motions. In other words, it could be speculated that the energy landscape of a protein could be evolved to assure the presence of several minima (high frustration), in order to assure a variety of different conformational states eventually leading

to the establishment of collective modes which could be essential to perform a given functional role.

CONCLUSIONS

The tumor suppressor p53 protein plays a crucial functional role in many cellular functions and it is characterized by a partial disordered character which is at the basis of its extremely intriguing dynamical behaviour. A computational approach was applied to investigate p53 and four mutants; each one containing a different punctual mutation located close to the DNA binding region. All atoms MD trajectories of wild-type p53 and its mutants, were analysed by focussing our attention on collective modes and on the degeneracy of the energy landscape. An analysis by ED method revealed the establishment of collective modes in p53, with a large involvement of regions containing the binding sites of physiological ligands; this providing a support for strong connection of collective modes and functionality. As consequence of punctual mutations, some collective motions of p53 undergo a drastic reduction, at the same time, the emergence of new collective motions were observed. These results indicate that a punctual mutation is able to affect the global behaviour of the p53 molecule, eventually leading to a new functionality, consistent with the GOF picture. An analysis of the MD results by applying the frustration a method indicated: i) regions with high frustration are the same largely involved in collective motions; ii) punctual mutation can significantly modulate frustration even of regions far from the mutations. These results provide some hints to understand the basic mechanisms regulating p53 whose structural and dynamical complexity has a direct consequence on its intricate functional role. Furthermore, they provide some clues on how to modify the functionality of a biomolecule through a punctual mutation leading to an appropriate modulation of the energy landscape.

Acknowledgments: ARB would like to thank Prof. Salvatore Cannistraro for fruitful discussion and evaluable suggestions.

Conflicts of Interest: The author declares no conflict of interest

REFERENCES

(1) Vogelstein, B.; Lane, D.; Levine, a J. Surfing the p53 network.*Nature* 2000, *408* (6810), 307–310 DOI: 10.1038/35042675.

(2) Cañadillas, J. M. P.; Tidow, H.; Freund, S. M. V; Rutherford, T. J.; Ang, H. C.; Fersht, A. R. Solution structure of p53 core domain: structural basis for its instability. *Proc. Natl. Acad. Sci. U. S. A.* 2006, *103* (7), 2109–2114 DOI: 10.1073/pnas.0510941103.

(3) Pagano, B.; Jama, A.; Martinez, P.; Akanho, E.; Bui, T. T. T.; Drake, A. F.; Fraternali, F.; Nikolova, P. V. Structure and stability insights into tumour suppressor p53 evolutionary related proteins.*PLoS One* 2013, *8* (10), e76014 DOI: 10.1371/journal.pone.0076014.

(4) Bell, S.; Klein, C.; Mueller, L.; Hansen, S.; Buchner, J. P53 Contains Large Unstructured Regions in Its Native State. *J. Mol. Biol.* 2002, *322* (5), 917–927 DOI: 10.1016/S0022-2836(02)00848-3.

(5) Cho, Y.; Gorina, S.; Jeffrey, P. D.; Pavletich, N. P. Crystal structure of a p53 tumor suppressor-DNA complex: understanding tumorigenic mutations. *Science* 1994, *265* (5170), 346–355 DOI: 10.1126/science.8023157.

(6) Fernandez-Fernandez, M. R.; Sot, B. The relevance of protein-protein interactions for p53 function: The CPE contribution. *Protein Eng. Des. Sel.* 2011, *24* (1–2), 41–51 DOI: 10.1093/protein/gzq074.

(7) Bizzarri, A. R.; Cannistraro, S. Direct interaction of miRNA and circRNA with the oncosuppressor p53: An intriguing perspective in cancer research. *Cancers (Basel).* 2021, *13* (23) DOI: 10.3390/cancers13236108.

(8) Vousden, K. H.; Lane, D. P. p53 in health and disease. *Nat. Rev. Mol. Cell Biol.* 2007, *8* (4), 275–283 DOI: 10.1038/nrm2147.

(9) Merkel, O.; Taylor, N.; Prutsch, N.; Staber, P. B.; Moriggl, R.; Turner, S. D.; Kenner, L. When the guardian sleeps: Reactivation of the p53 pathway in cancer. *Mutat. Res.* 2017, *773* , 1–13 DOI:

10.1016/j.mrrev.2017.02.003.

(10) Muller, P. A. J.; Vousden, K. H. Mutant p53 in Cancer: New Functions and Therapeutic Opportunities. *Cancer Cell* 2014,*25* (3), 304–317 DOI: 10.1016/j.ccr.2014.01.021.

(11) Friedler, A.; Hansson, L. O.; Veprintsev, D. B.; Freund, S. M. V.; Rippin, T. M.; Nikolova, P. V.; Proctor, M. R.; Rüdiger, S.; Fersht, A. R.; Rudiger, S.; et al. A peptide that binds and stabilizes p53 core domain: chaperone strategy for rescue of oncogenic mutants. *Proc. Natl. Acad. Sci. U. S. A.* 2002, *99* (2), 937–942 DOI: 10.1073/pnas.241629998.

(12) Oren, M.; Rotter, V. Mutant p53 gain-of-function in cancer.*Cold Spring Harb. Perspect. Biol.* 2010, *2* (2), a001107–a001107 DOI: 10.1101/cshperspect.a001107.

(13) Oldfield, C. J.; Dunker, A. K. Intrinsically Disordered Proteins and Intrinsically Disordered Protein Regions. *Annu. Rev. Biochem.*2014, *83* (1), 553–584 DOI: 10.1146/annurev-biochem-072711-164947.

(14) Habchi, J.; Tompa, P.; Longhi, S.; Uversky, V. N. Introducing Protein Intrinsic Disorder. *Chem. Rev.* 2014, *114* (13), 6561–6588 DOI: 10.1021/cr400514h.

(15) Berlow, R. B.; Dyson, H. J.; Wright, P. E. Functional advantages of dynamic protein disorder. *FEBS Lett.* 2015, *589* (19 Pt A), 2433–2440 DOI: 10.1016/j.febslet.2015.06.003.

(16) Huang, Y.; Liu, Z. Kinetic advantage of intrinsically disordered proteins in coupled folding-binding process: a critical assessment of the "fly-casting" mechanism. *J. Mol. Biol.* 2009, *393*(5), 1143—1159 DOI: 10.1016/j.jmb.2009.09.010.

(17) Frauenfelder, H.; Parak, F., Young, R. D. Conformational substates in proteins. *Ann. Rev. Biophys. Biophys.Chem.* 1988, *17* , 451–479.

(18) Frauenfelder, H.; Chen, G.; Berendzen, J.; Fenimore, P. W.; Jansson, H.; McMahon, B. H.; Stroe, I. R.; Swenson, J.; Young, R. D. A unified model of protein dynamics. *Proc. Natl. Acad. Sci. U. S. A.* 2009, *106* (13), 5129–5134 DOI: 10.1073/pnas.0900336106.

(19) Frauenfelder, H.; Sligar, S. G.; Wolynes, P. G. The energy landscapes and motions of proteins. *Science (80-.).* 1991,*254* (5038), 1598–1603 DOI: 10.1126/science.1749933.

(20) Ferreiro, D. U.; Hegler, J. A.; Komives, E. A.; Wolynes, P. G. Localizing frustration in native proteins and protein assemblies.*Proc. Natl. Acad. Sci. U. S. A.* 2007, *104* (50), 19819–19824 DOI: 10.1073/pnas.0709915104.

(21) Fong, J. H.; Shoemaker, B. A.; Garbuzynskiy, S. O.; Lobanov, M. Y.; Galzitskaya, O. V.; Panchenko, A. R. Intrinsic disorder in protein interactions: Insights from a comprehensive structural analysis.*PLoS Comput. Biol.* 2009, *5* (3), 13–17 DOI: 10.1371/journal.pcbi.1000316.

(22) Chillemi, G.; Davidovich, P.; Abramo, M. D.; Mametnabiev, T.; Garabadzhiu, A. V.; Desideri, A.; Melino, G. Molecular dynamics of the full - length p53 monomer. 2013, *12* (18), 3098–3108.

(23) Ferreiro, D.U.; Hegler, J.A.; Komives,E.A.; Wolynes, P.G. On the role of frustration in the energy landscapes of allosteric proteins. *Proc. Natl. Acad. Sci.* **2011** , *108* (9), 3499–3503 DOI: 10.1073/pnas.1018980108.

(24) Leroy, B.; Fournier, J. L.; Ishioka, C.; Monti, P.; Inga, A.; Fronza, G.; Soussi, T. The TP53 website: an integrative resource centre for the TP53 mutation database and TP53 mutant analysis. *Nucleic Acids Res.* **2013** , *41* (D1), D962–D969 DOI: 10.1093/nar/gks1033.

(25) Joerger, A. C.; Fersht, A. R. The p53 Pathway: Origins, Inactivation in Cancer, and Emerging Therapeutic Approaches. *Annu. Rev. Biochem.* **2016** , *85* , 375–404 DOI: 10.1146/annurev-biochem-060815-014710.

(26) Muller, P. A. J.; Caswell, P. T.; Doyle, B.; Iwanicki, M. P.; Tan, E. H.; Karim, S.; Lukashchuk, N.; Gillespie, D. A.; Ludwig, R. L.; Gosselin, P.; et al. Mutant p53 Drives Invasion by Promoting Integrin Recycling. *Cell* **2009** , *139* (7), 1327–1341 DOI: https://doi.org/10.1016/j.cell.2009.11.026.

(27) Walerych, D.; Lisek, K.; Del Sal, G. Mutant p53: One, No One, and One Hundred Thousand. *Front. Oncol.* **2015** , *5* , 289 DOI: 10.3389/fonc.2015.00289.

(28) Grugan, K. D.; Vega, M. E.; Wong, G. S.; Diehl, J. A.; Bass, A. J.; Wong, K. K.; Nakagawa, H.; Rustgi, A. K. A common p53 mutation (R175H) activates c-Met receptor tyrosine kinase to enhance tumor cell invasion.*Cancer Biol. Ther.* **2013** , *14* (9), 853–859 DOI: 10.4161/cbt.25406.

(29) Chiang, Y.-T.; Chien, Y.-C.; Lin, Y.-H.; Wu, H.-H.; Lee, D.-F.; Yu, Y.-L. The Function of the Mutant p53-R175H in Cancer. *Cancers* . 2021.

(30) Pilley, S.; Rodriguez, T. A.; Vousden, K. H. Mutant p53 in cell-cell interactions. *Genes Dev.* **2021** , *35* (7), 433–448 DOI: 10.1101/gad.347542.120.

(31) Chiang, Y.-T.; Chien, Y.-C.; Lin, Y.-H.; Wu, H.-H.; Lee, D.-F.; Yu, Y.-L.; Grugan, K. D.; Vega, M. E.; Wong, G. S.; Diehl, J. A.; et al. The Function of the Mutant p53-R175H in Cancer. *Cancer Biol. Ther.***2021** , *14* (7), D962–D969 DOI: 10.4161/cbt.25406.

(32) Seagle, B.-L. L.; Eng, K. H.; Dandapani, M.; Yeh, J. Y.; Odunsi, K.; Shahabi, S. Survival of patients with structurally-grouped TP53 mutations in ovarian and breast cancers. *Oncotarget; Vol 6, No 21***2015** .

(33) Yang, D. S.; Saeedi, A.; Davtyan, A.; Fathi, M.; Sherman, M. B.; Safari, M. S.; Klindziuk, A.; Barton, M. C.; Varadarajan, N.; Kolomeisky, A. B.; et al. Mesoscopic protein-rich clusters host the nucleation of mutant p53 amyloid fibrils. *Proc. Natl. Acad. Sci. U. S. A.* **2021** , *118* (10) DOI: 10.1073/pnas.2015618118.

(34) Kuo, W. C.; Sarangadharan, I.; Pulikkathodi, A. K.; Chen, P. H.; Wang, S. L.; Wu, C. R.; Wang, Y. L.; Wang, H. H.; Wang, H. H.; Zhang, M.; et al. Gold nanoparticles-decorated graphene field-effect transistor biosensor for femtomolar MicroRNA detection. *Anal. Chem.***2019** , *91* (9), 1–9 DOI: 10.1038/s41598-018-20229-z.

(35) Zhang, Y.; Coillie, S. V.; Fang, J. Y.; Xu, J. Gain of function of mutant p53: R282W on the peak? *Oncogenesis* **2016** ,*5* (October 2015), 2–5 DOI: 10.1038/oncsis.2016.8.

(36) Roy, A.; Kucukural, A.; Zhang, Y. I-TASSER: A unified platform for automated protein structure and function prediction. *Nat. Protoc.***2010** , *5* (4), 725–738 DOI: 10.1038/nprot.2010.5.

(37) Yang, J.; Zhang, Y. I-TASSER server: New development for protein structure and function predictions. *Nucleic Acids Res.***2015** , *43* (W1), W174–W181 DOI: 10.1093/nar/gkv342.

(38) Duan, J.; Nilsson, L. Effect of Zn2+ on DNA recognition and stability of the p53 DNA-binding domain. *Biochemistry***2006** , *45* (24), 7483–7492 DOI: 10.1021/bi0603165.

(39) Calimet, N.; Simonson, T. Cys_xHis_y-Zn^{2+} interactions: Possibilities and limitations of a simple pairwise force field. *J. Mol. Graph.* **2006** ,*24* , 404–411.

(40) Grandis, V. De; Bizzarri, A. R.; Cannistraro, S.; Docking study and free energy simulation of the complex between p53 DNA-binding domain and azurin. *J. Mol. Recognit.* **2007** , *20* (4), 215–226 DOI: 10.1002/jmr.840.

(41) Bizzarri, A. R.; Santini, S.; Coppari, E.; Bucciantini, M.; Di Agostino, S.; Yamada, T.; Beattie, C. W.; Cannistraro, S. Interaction of an anticancer peptide fragment of azurin with p53 and its isolated domains studied by atomic force spectroscopy. *Int. J. Nanomedicine* **2011** , *6* (1), 3011–3019 DOI: 10.2147/IJN.S26155.

(42) Bizzarri, A. R.; Moscetti, I.; Cannistraro, S. BBA - General Subjects Interaction of the anticancer p28 peptide with p53-DBD as studied by fl uorescence , FRET , docking and MD simulations. *BBA - Gen. Subj.*

2019 , *1863* (2), 342–350 DOI: 10.1016/j.bbagen.2018.11.003.

(43) Guex, N.; Peitsch, M. C. SWISS-MODEL and the Swiss-PdbViewer: An environment for comparative protein modeling. *Electrophoresis***1997** , *18* (15), 2714–2723.

(44) Abraham, M. J.; Murtola, T.; Schulz, Roland Shultz, S. P.; Smith, J. C.; Hess, B.; Lindah, E. Gromacs: High performance molecular simulations through multi-level parallelism from laptops to supercomputers. *SoftwareX* **2015** , *1 –2* , 19–25 DOI: 10.1016/j.softx.2015.06.001.

(45) Ponder, J. W.; Case, D. A. Force Fields for Protein Simulations. In*Protein Simulations* ; Academic Press, 2003; Vol. 66, pp 27–85.

(46) Berendsen, H. J. C.; Grigera, J. R.; Straatsma, T. P. The missing term in effective pair potentials. *J. Chem. Phys.* **1981** ,*91* (24), 6269–6271 DOI: 10.1021/j100308a038.

(47) Santini, S.; Bizzarri, A. R.; Cannistraro, S. Modelling the interaction between the p53 DNA-binding domain and the p28 peptide fragment of Azurin. *J. Mol. Recognit.* **2011** , *24*(6) DOI: 10.1002/jmr.1153.

(48) Hess, B.; Bekker, H.; Berendsen, H. J. C.; Fraaije, J. G. E. M. LINCS: A linear constraint solver for molecular simulations. *J. Comput. Chem.* **1997** , *18* (12), 1463–1472 DOI: 10.1002/(SICI)1096-987X(199709)18:12<1463::AID-JCC4>3.0.CO;2-H.

(49) Kholmurodov, K.; Smith, W.; Yasuoka, K.; Darden, T.; Ebisuzaki, T. A smooth-particle mesh Ewald method for DL_POLY molecular dynamics simulation package on the Fujitsu VPP700. *J. Comput. Chem.***2000** , *21* (13), 1187–1191 DOI: 10.1002/1096-987X(200010)21:13<1187::AID-JCC7>3.0.CO;2-7.

(50) Darden, T.; York, D.; Pedersen, L. Particle mesh Ewald: An N[?]log(N) method for Ewald sums in large systems. *J. Chem. Phys.***1993** , *98* (12), 10089–10092 DOI: 10.1063/1.464397.

(51) Nose, S. A unified formulation of the constant temperature molecular dynamics methods. *J. Chem. Phys.* **1984** ,*81* (1), 511–519 DOI: 10.1063/1.447334.

(52) Parrinello, M.; Rahman, A. Polymorphic transitions in single crystals: A new molecular dynamics method. *J. Appl. Phys.***1981** , *52* (12), 7182–7190 DOI: 10.1063/1.328693.

(53) Eisenhaber, F.; Lijnzaad, P.; Argos, P.; Sander, C.; Scharf, M.; F. Eisenhaber, P. Lijnzaad, P. Argos, C. Sander, and M. S. The Double Cubic Lattice Method: Efficient Approaches to Numerical Integration of Surface Area and Volume and to Dot Surface Contouring of Molecular Assemblies.*J. Comput. Chem.* **1995** , *16* , 273–284 DOI: 10.1002/jcc.540160303.

(54) Humphrey, W. F.; Dalke, A.; Schulten, K. VMD—visual molecular dynamics. *J. Mol. Graph.* **1996** , *14* , 33–38.

(55) Amadei, A.; Linssen, A. B. M.; de Groot, B. L.; van Aalten, D. M. F.; Berendsen, H. J. C. An Efficient Method for Sampling the Essential Subspace of Proteins. *J. Biomol. Struct. Dyn.* **1996** ,*13* (4), 615–625 DOI: 10.1080/07391102.1996.10508874.

(56) de Groot, B. L.; Amadei, A.; van Aalten, D. M. F.; Berendsen, H. J. C. Towards an Exhaustive Sampling of the Configurational Spaces of the Two Forms of the Peptide Hormone Guanylin. *J. Biomol. Struct. Dyn.* **1996** , *13* (5), 741–751 DOI: 10.1080/07391102.1996.10508888.

(57) Amadei, A.; Linssen, A. B. M.; Berendsen, H. J. C. Essential dynamics of proteins. *Proteins Struct. Funct. Genet.***1993** , *17* (4), 412–425 DOI: 10.1002/prot.340170408.

(58) Jenik, M.; Parra, R. G.; Radusky, L. G.; Turjanski, A.; Wolynes, P. G.; Ferreiro, D. U. Protein frustratometer: a tool to localize energetic frustration in protein molecules. *Nucleic Acids Res.***2012** , *40* (Web Server issue), W348–W351 DOI: 10.1093/nar/gks447.

(59) Parra, R. G.; Schafer, N. P.; Radusky, L. G.; Tsai, M.-Y.; Guzovsky, A. B.; Wolynes, P. G.; Ferreiro, D. U. Protein Frustratometer 2: a tool to localize energetic frustration in protein molecules, now with electrostatics. *Nucleic Acids Res.* **2016** , *44*(W1), W356–W360 DOI: 10.1093/nar/gkw304.

(60) Bizzarri, A. R.; Cannistraro, S. Time-Resolved Fluorescence and Essential Dynamics Study on the Structural Heterogeneity of p53DBD Bound to the Anticancer p28 Peptide. *J. Phys. Chem. B* **2020** ,*124* (44), 9820–9828 DOI: 10.1021/acs.jpcb.0c06778.

(61) Blandino, G.; Di Agostino, S. New therapeutic strategies to treat human cancers expressing mutant p53 proteins. *J. Exp. Clin. Cancer Res.* **2018** , *37* (1), 30 DOI: 10.1186/s13046-018-0705-7.